Oxidative stress enhances and modulates protein S -nitrosation in smooth muscle cells exposed to S -nitrosoglutathione

E. Belcastro, W. Wu, I. Fries-Raeth, A. Corti, A. Pompella, P. Leroy, I. Lartaud, Caroline Gaucher

Oxidative stress enhances and modulates protein *S*-nitrosation in smooth muscle cells exposed to *S*-nitrosoglutathione

E. Belcastro[a, b], W. Wu[a], I. Fries-Raeth[a], A. Corti[b], A. Pompella[b], P. Leroy[a], I. Lartaud[a], C. Gaucher[a]*

[a]*Université de Lorraine, CITHEFOR EA 3452, Faculté de Pharmacie, BP 80403, F-54001 Nancy Cedex, France*

[b] *Department of Translational Research NTMS, University of Pisa Medical School, Via Roma 55, 56126 Pisa, Italy.*

* Corresponding author: Dr Caroline Gaucher. Université de Lorraine, CITHEFOR EA 3452, Faculté de Pharmacie, BP 80403, F-54001 Nancy Cedex, France.

E-mail address: caroline.gaucher@univ-lorraine.fr; Tel.: +33 3 72 74 73 49.

Abstract

Among *S*-nitrosothiols showing reversible binding between NO and -SH group, *S*-nitrosoglutathione (GSNO) represents potential therapeutics to treat cardiovascular diseases (CVD) associated with reduced nitric oxide (NO) availability. It also induces *S*-nitrosation of proteins, responsible for the main endogenous storage form of NO. Although oxidative stress parallels CVD development, little is known on the ability of GSNO to restore NO supply and storage in vascular tissues under oxidative stress conditions.

Aortic rat smooth muscle cells (SMC) were stressed *in vitro* with a free radical generator (2,2'-azobis(2-amidinopropane) dihydrochloride, AAPH). The cellular thiol redox status was reflected through levels of reduced glutathione and protein sufhydryl (SH) groups. The ability of GSNO to deliver NO to SMC and to induce protein *S*-nitrosation (investigated *via* mass spectrometry, MS), as well as the implication of two redox enzymes involved in GSNO metabolism (activity of gamma-glutamyltransferase, GGT, and expression of protein disulfide isomerase, PDI) were evaluated.

Oxidative stress decreased both intracellular glutathione and protein -SH groups (53% and 32% respectively) and caused a 3.5-fold decrease of GGT activity, while PDI expression at the plasma membrane was 1.7-fold increased without any effect on extracellular GSNO catabolism. Addition of GSNO (50 μM) increased protein -SH groups and protein *S*-nitrosation (50%). Mass spectrometry analysis revealed a higher number of *S*-nitrosated proteins under oxidative stress (83 proteins, *vs* 68 in basal conditions) including a higher number of cytoskeletal proteins (15, *vs* 9 in basal conditions) related with cell contraction, morphogenesis and movement. Furthermore, proteins belonging to additional protein classes (cell adhesion, transfer/carrier, and transporter proteins) were *S*-nitrosated under oxidative stress.

In conclusion, higher levels of GSNO-dependent *S*-nitrosation of proteins from the cytoskeleton and the contractile machinery were identified under oxidative stress conditions. The findings may prompt the identification of suitable biomarkers for the appraisal of GSNO bioactivity in the CVD treatment.

Keywords: Oxidative stress, *S*-nitrosoglutathione, Protein *S*-nitrosation, Gamma-glutamyltransferase, Protein disulfide isomerase, Mass spectrometry.

1. Introduction

Cardiovascular diseases like atherosclerosis, pulmonary hypertension, thrombosis, ischemia and cardiac arrhythmia are usually associated with oxidative stress and a reduced bioavailability of nitric oxide (NO) [1]. To overcome this aspect, several NO-related therapeutics have emerged over the past few decades, such as nitrosamines [2], organic nitrates [3], and N-diazeniumdiolates [4]. However, these compounds induce undesirable effects, such as tolerance and hypotension, and are often considered as oxidative stress enhancers in an environment rich in oxygen and/or radical species, where they may favour the formation of peroxynitrite ions ($ONOO^-$), a reactive nitrogen species (RNS) producing deleterious protein nitration [5, 6, 7, 8]. Other NO coumpounds, such as *S*-nitrosothiols may represent safer alternatives [9, 10]. Several investigations on the therapeutic potential of *S*-nitrosothiols have focused on *S*-nitrosoglutathione (GSNO), the physiological storage form of NO in tissues, due to the absence of recorded side effects in preclinical studies [11, 12, 13]. However, even though *S*-nitrosothiols are not prooxidant *per se,* the ability of GSNO to regulate NO bioavailability under oxidative stress conditions has not yet received sufficient attention.

Oxidative stress in the vessel wall has been shown to involve the *tunica media,* where smooth muscle cells (SMC) can produce reactive oxygen species (ROS) – *e.g.* superoxide anion, $O_2^{\bullet-}$– following the activation of their own NADPH oxidase. SMC probably represent a privileged target of ROS [14]. Exposure of SMC cells to ROS-generating systems actually stimulates migration, proliferation, and growth [15, 16, 17, 18]. SMC also are a main target of (endothelium-derived or exogenous) NO, which exerts in this way its vasorelaxing effects.

NO, besides its direct role in vascular function, also participates in redox signaling by modifying proteins *via S*-nitrosation. The *S*-nitrosation, which is the formation of a covalent bond between NO and the sulfhydryl group of a cysteine residue, is a redox dependent, thiol-

based, reversible posttranslational modification of proteins [19, 20, 21]. There are emerging data suggesting that *S*-nitrosation of proteins plays an important role both in physiology and in a broad spectrum of pathologies [22]. Pathophysiology correlates with hypo or hyper *S*-nitrosation level of specific protein targets. This dysregulation of protein *S*-nitrosation results from a modification of NO availability (quantity and/or localization). NO availability results not only from alterations of the expression, compartmentalization and/or activity of NO synthases, but also reflects the contribution of denitrosylases, including GSNO-metabolizing enzymes, like GSNO reductase releasing GSNHOH, a non active NO-related molecule, and the gamma-glutamyltransferase (GGT) releasing cys-gly-NO, an active NO-related molecule [23]. Redoxines like protein disulfide isomerase (PDI) known to reverse thiol oxidation can also catabolise GSNO to release NO [24].

In the present study, we aimed to assess the suitability and potency of GSNO as a NO donor in an oxidative stress environment. Its metabolism by two specific redox enzymes (GGT and PDI), the cellular thiol redox status and protein *S*-nitrosation were thus analyzed in SMC exposed to oxidative stress induced by a free radical generator, *i.e.* 2,2'-azobis(2-amidinopropane) dihydrochloride (AAPH). We more specifically evaluated whether oxidative stress modulates the bioactivity of GSNO, by favouring release of NO and *S*-nitrosation of potentially critical protein targets related with cell contraction, morphogenesis and movement.

2. Materials and methods

2.1. Materials

2.1.1. Chemicals

All reagents were of analytical grade and all solutions prepared with ultrapure deionized water (>18.2 mΩ.cm). The Bicinchoninic acid (BCA) protein assay kit was purchased from Pierce and protease inhibitor cocktail from Roche. The *N*-[6-

(biotinamido)hexyl]-3'-(2'-pyridyldithio)-propionamide biotin (Ez-Link Biotin-HPDP) and the high capacity neutravidin agarose resin were obtained from Fisher Scientific. All other reagents came from Sigma, France, country not precised for other companies.

2.1.2. Synthesis of S-nitrosoglutathione

GSNO was synthesized as previously described [25]. Briefly, reduced glutathione (GSH) was incubated with an equivalent amount of sodium nitrite under acidic conditions (0.626 M HCl). The concentration of GSNO was calculated using the specific molar absorbance of S-NO bond at 334 nm ($\varepsilon = 922\ M^{-1}cm^{-1}$) and the Beer-Lambert law.

2.2. Cell culture and oxidative stress model

Vascular smooth muscle cells derived from embryonic rat aorta (A-10 line, ATCC, USA) were grown in Dulbecco's modified Eagle's medium supplemented with 10% (v/v) fetal bovine serum, 4.5 g/L glucose, 2% (v/v) glutamine (200 mM), 100 U/mL penicillin, 100 µg/mL streptomycin, 1 mM sodium pyruvate, as well as phenol red. They were cultured at 37°C under 10% (v/v) CO_2 in a humidified incubator and used between passages 25 and 30. For all experiments, cells were seeded in a 6-wells plate at 6,400 cells/cm^2, 48 h before stimulation. Oxidative stress was induced on cells during 2 h at 37°C by addition of 50 mM 2,2'-azobis(2-amidinopropane) dihydrochloride (AAPH) in an incubation medium containing 5% (v/v) fetal bovine serum, 4.5 g/L glucose, 2% (v/v) glutamine (200 mM), 100 U/mL penicillin and 100 µg/mL streptomycin. After oxidative stress induction, 50 µM of GSNO (or the same volume of phosphate buffered saline, PBS) was added for an additional incubation period of 1 h at 37°C.

In another set of experiments, 15 min before the end of oxidative stress induction, 20 mM of serine borate complex (SBC), or 100 µM of bacitracin were added to inhibit GGT or PDI, respectively [23, 26].

2.3. S-nitrosoglutathione metabolism

2.3.1. Quantification of extracellular S-nitrosothiols

After cell incubation (see section 2.2.), media were collected for quantification of nitrite ions and total *S*-nitrosothiols (including residual GSNO) using the Griess and Griess-Saville methods. Briefly, 100 µL of sample were diluted with 100 µL acetoacetic solution 11% (v/v) (pH= 2.5). Then, for nitrite ions quantification, 40 µL of sulfanilamide solution in 0.4 M HCl were added (Griess assay). For *S*-nitrosothiols quantification, the sulfanilamide solution was supplemented with 0.2% (w/v) $HgCl_2$ (to cleave the S-NO bond: Griess-Saville assay). Finally, the diazonium salt formed was made to react with 10 µL of a 0.6% (w/v) *N*-(1-naphthyl) ethylenediamine solution to form a chromophoric azo product that absorbs at 540 nm. To calculate the concentration of *S*-nitrosothiols, free nitrite ions quantified by Griess assay were subtracted from those obtained with the Griess-Saville assay.

2.3.2. Quantification of intracellular S-nitrosothiols

Intracellular *S*-nitrosothiols were quantified by using the 2,3-diaminonaphthalene (DAN) fluorogenic probe (this assay offers a lower limit of quantification than the Griess method). After incubation (see section 2.2.), cells were washed with PBS and lysed with 500 µL of 0.4% (w/v) Triton X-100 in 0.1 M HCl. The intracellular *S*-nitrosated proteins were quantified by the DAN (nitrite ions) or DAN-Hg^{2+} (*S*-nitrosothiols) assays using standard curves (0.1 - 1 µM) of sodium nitrite and GSNO, respectively [27]. The concentration of nitrite ions (DAN assay) was subtracted from the DAN-Hg^{2+} quantification to obtain the intracellular *S*-nitrosothiols concentration, which was normalized upon the intracellular protein concentration (see section 2.7).

2.4. Thiol redox status

The redox potential of the culture medium was measured by using a redox electrode (Hanna Instruments) combined with a reference Ag/AgCl electrode (E = +0.207 V)**.**

2.4.1. Quantification of reduced membrane thiols

After incubation, media were withdrawn and cells washed twice (PBS). Cells were then incubated for 10 min in the dark with 750 µL of 1 mM 5-5'-dithio-bis(2-nitrobenzoic) acid (DTNB) prepared in PBS. Then, 200 µL from each well were transferred in triplicate in a 96-wells plate and absorbance read at 405 nm (EL800, Universal Microplate Reader, BioTek Instruments). Membrane thiols concentration was calculated using a GSH standard curve ranging from 3.25 µM to 32.5 µM and expressed relatively to protein content (see section 2.7).

2.4.2. Quantification of intracellular reduced glutathione

Intracellular GSH was measured as previously described [28, 29], with some adaptations. Cells were lysed in a cold 3.3 % (v/v) perchloric acid solution and centrifuged for 15 min at 10,000 ×*g*. Acidic supernatants were neutralized with 10 M NaOH and diluted 10 times in 0.1 M HCl containing 2 mM ethylenediaminetetraacetic acid (EDTA). Sixty µL of diluted samples or standard GSH solutions (0.65–3.25 µM) were transferred to a 96-wells microplate; 120 µL of 0.4 M borate buffer (pH = 9.2) and 20 µL of 5.4 mM 2,3-naphthalene dicarboxaldehyde (NDA) solution prepared in ethanol were then added into each well. The microplate was incubated for 25 min on ice in the dark. The fluorescence intensity of GSH-NDA adducts was measured using a microplate reader (Synergy 2 model, Biotek Instruments, Colmar, France) with excitation set at 485 ± 20 nm and emission at 528 ± 20 nm and expressed relatively to protein content (see section 2.7).

2.4.3. Quantification of intracellular protein reduced thiols

Intracellular protein reduced thiols were quantified using the DTNB method. After treatments, cells were lysed in a 3.3% (v/v) cold perchloric acid solution and centrifuged for 15 min at 10,000 × *g*. The pellets were resuspended in PBS containing 0.5% (V/V) sodium dodecylsulfate (SDS) and the resulting suspensions were incubated for 10 min in the dark after adding 700 µL of 1 mM DTNB. Then, 200 µL of each suspension were transferred in triplicate into a 96-wells microplate and the absorbance was read at 405 nm. Intracellular thiol concentrations were calculated using a GSH standard curve ranging from 3.25 µM to 32.5 µM and expressed relatively to protein content (see section 2.7).

2.5. Determination of gamma-glutamyltransferase activity

Gamma-glutamyltransferase activity was kinetically determined using the synthetic GGT substrate L-gamma-glutamyl-3-carboxy-4-nitroanilide (GCNA). After treatments, incubation media were replaced with 750 µL of 1 mM-GCNA in 100 mM Tris buffer (pH= 7.4) containing 20 mM glycyl-glycine and 10 mM $MgCl_2$, with/without 50 mM AAPH or 20 mM of the GGT inhibitor SBC. Cells were then incubated at 37°C, and 50 µL of the incubation medium were transferred into a 96-wells microplate every 30 min, and the absorbance was read at 405 mm. At the end of the kinetic assay, cells were lysed in 500 µL 0.1 M HCl containing 0.4% (m/v) Triton X-100 for protein quantification (see section 2.7).

2.6. Cell membrane PDI expression

2.6.1. Western blot analysis

Cells were scraped in 50 mM Tris buffer (pH= 8) added with 50 mM 2-mercaptoethanol and protease inhibitor cocktail (Roche, France). After 30-min incubation on ice, cell lysates were centrifuged at 17,600 × *g* during 20 min. The pellet containing

membrane proteins was resuspended in 50 mM Tris buffer (pH= 8) added with 1% (v/v) SDS and agitated for 30 min on ice. Membrane proteins were then centrifuged for 20 min at 21,000 × *g*. Finally, proteins were precipitated with 100% cold acetone for 1 h at -20°C. After centrifugation (3,000 × *g*, 10 min), the pellet was resuspended in 50 mM Tris buffer (pH= 6.8) containing 0.15 M NaCl, 1% (w/v) SDS and 1% (w/v) Triton X-100. Proteins were quantified (see section 2.7) and 10 µg were deposited on a SDS PAGE with 10% separative gel and 4% concentrating gel. After migration, proteins were transferred onto a polyvinyl membrane and labelled with anti-PDI (sc-20132 Santa Cruz biotechnology) or anti-actin antibody diluted 1/1000 and 1/2000, respectively. Secondary antibody conjugated with horseradish peroxidase (sc-2004, Santa Cruz biotechnology) diluted 1/5000 was used to quantify PDI/actin ratio using the Image J 1.47V software (NIH, USA).

2.6.2. Confocal microscopy imaging

Cells were fixed during 30 min with 4% (w/v) paraformaldehyde then incubated 45 min at room temperature with the anti PDI primary monoclonal antibody (sc-20132 Santa Cruz biotechnology) diluted at 1/50 in PBS/0.5% bovine serum albumin (BSA). After two washing with PBS/0.5% (w/v) BSA, cells were incubated 45 min at room temperature with the secondary antibody, polyclonal goat anti rabbit immunoglobulin G coupled to CF 488 (Sigma, France) diluted to 1/100 in PBS/0.5% (w/v) BSA. Then, cells were permeabilized with Triton X-100 (0.4%, w/v) during 15 min in order to couterstain nuclei with To-Pro®-3 (Life technologies).

2.7. Total protein quantification

Protein determination was performed using the Pierce BCA Protein Assay Kit, following instructions of the manufacturer. A standard curve ranging from 0.025 to 1 $mg.mL^{-1}$ was built with bovine serum albumin to calculate protein concentration.

2.8. Purification and identification of S-nitrosated cysteine residues in proteins

Cells incubated in a-75 cm^2 flask were lysed in 500 µL of 50 mM Tris (pH= 6.8) buffer containing 0.15 M NaCl, 1% (v/v) NP-40, 0.1% (v/v) SDS, 1mM EDTA, 0.1mM neocuproine and protease inhibitor cocktail. *S*-nitrosated proteins were purified by the biotin switch technique as previously described [30, 31], with some adaptations. Briefly, free thiols in cell lysates were blocked with 50 mM of *N*-ethylmaleimide (NEM). Then, *S*-nitrosated proteins were labeled with biotin-HPDP after S-NO bond cleavage with sodium ascorbate. Then proteins were digested overnight with sequencing-grade trypsin (Promega) at a 1:100 (w:w) trypsine:protein ratio. Trypsine activity was stopped by addition of 500 mM of phenylmethylsulfonyl fluoride (PMSF). Biotin-HPDP-labeled protein digests were purified with NeutrAvidin beads (High Capacity NeutrAvidinAgarose Resin) and eluted in a buffer containing 1.5% (v/v) 2-mercaptoethanol.

After purification, *S*-nitrosated protein digests were identified by mass spectrometry, as follows. ~~Samples diluted 4-fold in 6 M urea, 50 mM Tris (pH= 8.0) were processed for cysteine reduction and alkylation, followed by overnight digestion in 10 vol of 50 mM Tris (pH= 8.0), 1 mM $CaCl_2$ containing 100 ng sequencing-grade trypsin (Promega)~~. Protein digests were purified through C18 mini spin columns (Pierce, Thermofisher scientific, France), resuspended in 8 µL of 2% (v/v) acetonitrile, 0.1% (v/v) trifluoroacetic acid and analyzed through label-free liquid chromatography coupled to matrix-assisted laser desorption/ionization (LC-MALDI) as previously described [32]. Proteins and peptides were identified based on fragmentation spectra by interrogation of the whole Swissprot database through the public Mascot server (taking in account ~~protein scores above 80.0 and~~ peptide scores above 50.0 at first rank, allowing one trypsin miscleavage and considering cysteine

carbamidomethylation and methionine oxidation as optional). Finally, identified proteins were classified using the Panther database [33].

2.9. Statistical analysis of data

Results are expressed as means ± standard error of the mean (sem). Statistical analyses were performed using either the Student t-test (for enzyme activity/expression or inhibition) or two-way ANOVA ($p_{condition}$basal *versus* AAPH, $p_{treatment}$with or without GSNO and $p_{interaction}$ between condition and treatment) followed by a Bonferroni's multiple comparisons test. The GraphPad Prism software (GraphPad Software version 5.0, San Diego, USA) was used.

3. Results

3.1. Validation of oxidative stress and S-nitrosation parameters of the cell model

The concentration of AAPH and GSNO used within this study were chosen upon the measurement of intracellular GSH concentration and intracellular formation of *S*-nitrosothiols, respectively (**Fig. 1**). A 2-h incubation period of SMC in the presence of 50 mM AAPH significantly decreased (two times compared to the basal condition) the intracellular concentration of GSH without altering cell viability (90 ± 2 % using the 3-(4,5-dimethylthiazol-2-yl)-2,5-diphenyltetrazolium bromide dye, MTT test) (**Fig. 1-A**). The GSNO concentration was fixed at 50 µM as the first effective concentration inducing significant intracellular *S*-nitrosothiols formation after a 1-h contact compared to basal condition (**Fig. 1-B**).

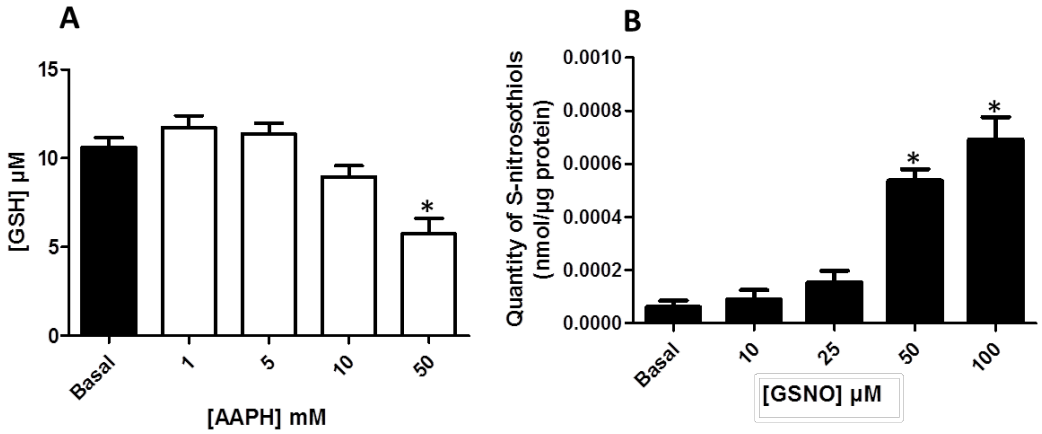

Fig. 1. Validation parameters of the cell model. (**A**) Smooth muscle cells were incubated for 2 h with different concentrations of AAPH. Intracellular concentration of GSH was quantified by the NDA assay. (**B**) Smooth muscle cells under basal conditions were incubated for 1 h with different GSNO concentrations. Intracellular *S*-nitrosothiols content was quantified by the DAN-Hg^{2+} method. Results are presented as means ± sem of three independent experiments and compared using a one way ANOVA. * $p < 0.05$ (Bonferroni's multiple comparisons test).

Furthermore, under oxidative stress, the GGT activity decreased 3.5 fold, from 1.35 ± 0.20 to 0.39 ± 0.14 nmol/min/mg of proteins (n = 3, Student t test, $p < 0.05$). At variance, the level of PDI localization in membranes including plasma and organelle membrane increased 1.7 fold, from 0.72 ± 0.02 to 1.22 ± 0.31 (PDI/actin ratio, n = 4, Student t-test, $p < 0.05$). Representative images showed a weak expression of PDI at cell plasma membrane under basal condition (**Fig. 2-A**) and a small but proven increase of PDI expression under oxidative stress (**Fig. 2-B**). These images showed about 10% of cells expressing PDI at their plasma membrane under oxidative stress (**Fig. 2-B**)

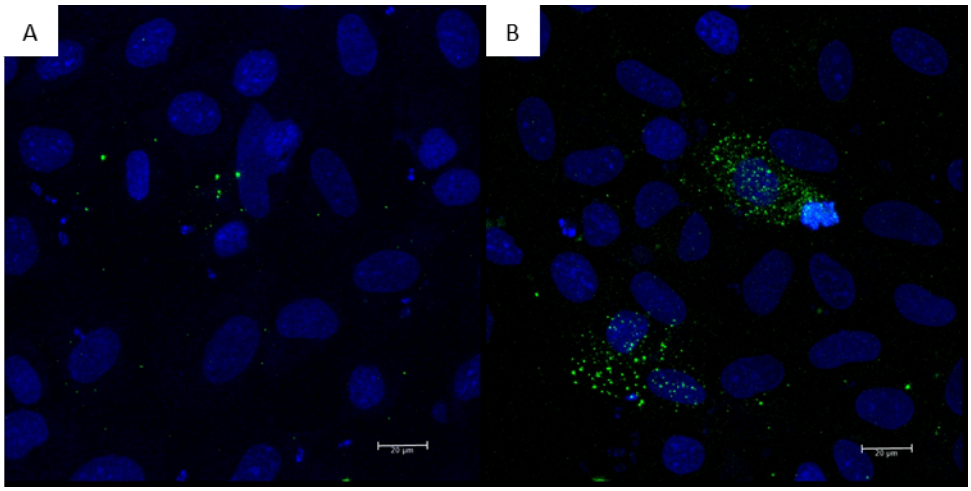

Fig. 2. PDI expression at plasma membrane of smooth muscle cells. Cells under basal (A) or oxidative stress (B) conditions were immunostained with anti PDI antibody and polyclonal goat anti rabbit immunoglobulin G coupled to CF 488. Nuclei were counterstained with To-Pro®-3. Representative confocal microscope images were taken with a 40x magnification and a numerical aperture of 0.8. n = 2

So, the present study explored the impact of GSNO incubated for a 1-h period after a 2-h period of oxidative stress induction leading to a total of 3-h of incubation.

3.2. Oxidative stress biomarkers

A 3-h incubation of SMC in presence of 50 mM AAPH significantly increased the redox potential of the culture medium from +256 ± 19 (basal) to +484 ± 8 mV (n = 3, Student t test, $p < 0.05$ *vs* basal). Addition of GSNO (50 µM) during the final 1-h incubation period had no impact on this redox potential, neither in control nor under AAPH exposure. No variation of the pH value (7.4) was observed all along the experiment.

The intracellular GSH content significantly decreased with oxidative stress **(Fig. 3-A**), while extracellular GSH increased **(Fig. 3-B)** ($p_{condition} < 0.0001$ for both). The addition of GSNO very slightly (1.9 %) but significantly increase the extracellular GSH ($p_{treatment} = 0.0395$), both in basal and oxidative conditions ($p_{interaction}$ ns), while did not allow the recovery of intracellular GSH level, which remained at a low value under AAPH exposure ($p_{treatment}$ and $p_{interaction}$ ns, **Fig. 3-A**).

Reduced thiols at the plasma membrane (0.015 ± 0.002 nmol/µg of proteins) did not change with oxidative stress. Intracellular protein thiols decreased with oxidative stress in the absence of GSNO, while the addition of GSNO almost doubled the intracellular protein thiol content under oxidative stress ($p_{interaction}$< 0.0007, **Fig. 3-C**).

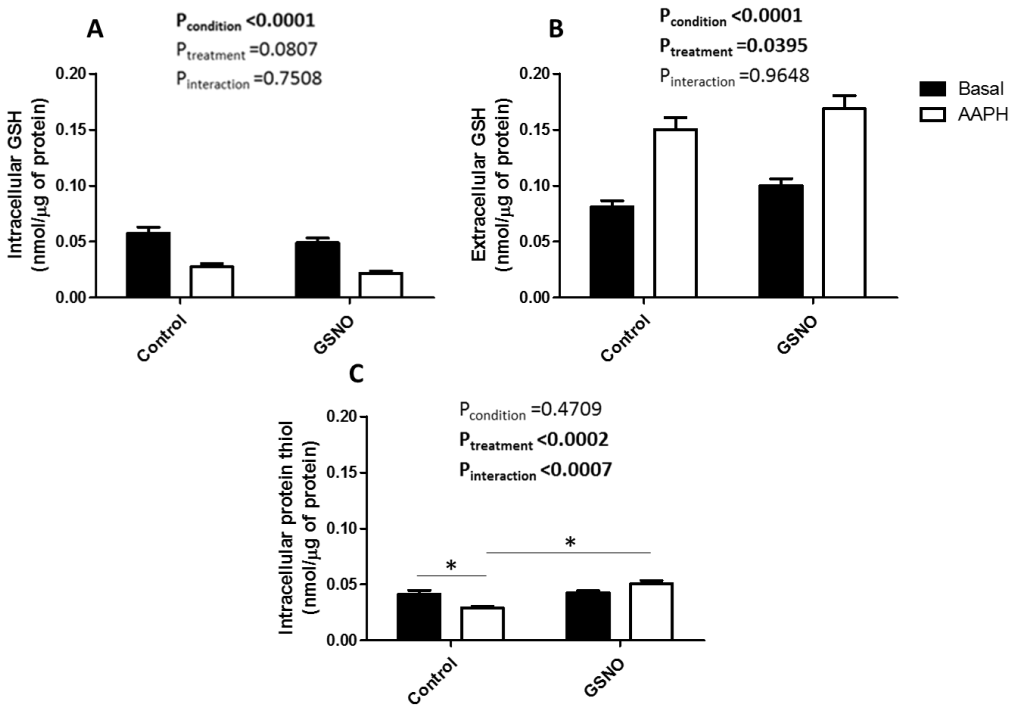

Fig. 3. Intracellular and extracellular thiol status in basal and oxidative stress conditions. Smooth muscle cells were incubated for a total of 3 h without (basal) or with 50 mM AAPH. In each condition, 50 µM GSNO or GSNO+AAPH were added during the 3rd h of incubation. Intracellular reduced thiols **(C)** were quantified by reacting precipitated proteins with DTNB. Intracellular **(A)** and extracellular GSH **(B)** were quantified with the NDA assay in the supernatant resulting from protein precipitation. Results are presented as means ± sem of three independent experiments and compared using a two way ANOVA ($p_{condition}$ (Basal *vs* AAPH), $p_{treatment}$ (Control, GSNO) and $p_{interaction}$); * $p < 0.05$ (Bonferroni's multiple comparisons test).

3.3. Extracellular GSNO metabolism and intracellular formation of S-nitrosothiols.

After 1-h contact with cells, only *ca.* 20 µM of GSNO **(Fig. 4-A)** – out of the 50 µM initially added, and *ca.* 12 µM of nitrite ions **(Fig. 4-B)** were measured in the extracellular

space, indicating that GSNO is partly metabolized by SMC to release NO (detected as nitrite ions).

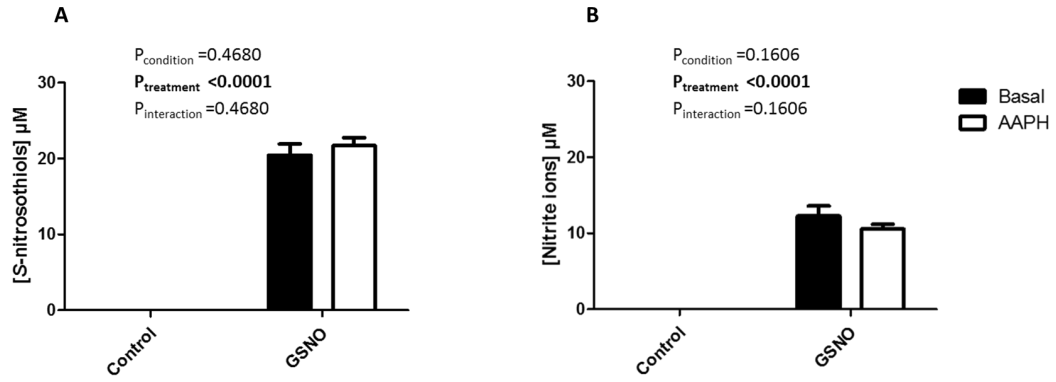

Fig. 4. Extracellular metabolism of *S*-nitrosoglutathione. Smooth muscle cells were incubated for 3 h without (basal) or with 50mM AAPH. In each condition, 50 µM GSNO or GSNO+AAPH were added during the 3rd hour of incubation. *S*-nitrosothiols **(A)** and nitrite ions **(B)** were quantified by the Griess-Saville and Griess methods, respectively. Results are presented as means ± sem of three independent experiments and compared using a two way ANOVA ($p_{condition}$ (Basal *vs* AAPH), $p_{treatment}$ (Control, GSNO) and $p_{interaction}$).

GGT and PDI inhibition under basal conditions led to an increased extracellular content of GSNO to 27 ± 0.5 µM for SBC and 28 ± 0.5 µM for bacitracin ($p < 0.05$ *versus* GSNO in the absence of inhibition, t-test) and a decrease in extracellular nitrite ions concentrations (10 ± 0.4 µM for SBC ($p > 0.05$) and 7 ± 0.9 µM for bacitracin ($p < 0.05$ *versus* GSNO in the absence of inhibition, t-test), attesting a decrease in GSNO catabolism. Similar profiles were obtained with GGT and PDI inhibition under oxidative stress.

At the intracellular level, cell exposure to GSNO for 1 h induced formation of *S*-nitrosothiols, which nearly doubled under oxidative stress compared to the basal condition **(Fig. 5)**. Both enzymes were implicated in the formation of intracellular *S*-nitrosothiols in both conditions. Inhibition of GGT by SBC led to a half time decrease of the *S*-nitrosothiols content, both in basal condition ($2.1.10^{-4} \pm 0.2.10^{-4}$ nmol/ µg of proteins, $p < 0.05$ *versus* GSNO in the absence of inhibition, t-test) and under oxidative stress ($6.6.10^{-4} \pm 0.4.10^{-4}$ nmol/ µg of proteins, $p < 0.05$ *versus* GSNO in the absence of inhibition, t-test). PDI inhibition by

bacitracin showed the same profile with a *S*-nitrosothiols formation decreasing to $2.90.10^{-4} \pm 0.05.10^{-4}$ nmol/µg of proteins in basal condition ($p < 0.05$ *versus* GSNO in the absence of inhibition, t-test) and to $4.5.10^{-4} \pm 0.5.10^{-4}$ nmol/µg of proteins under oxidative stress ($p < 0.05$ *versus* GSNO in the absence of inhibition, t-test).

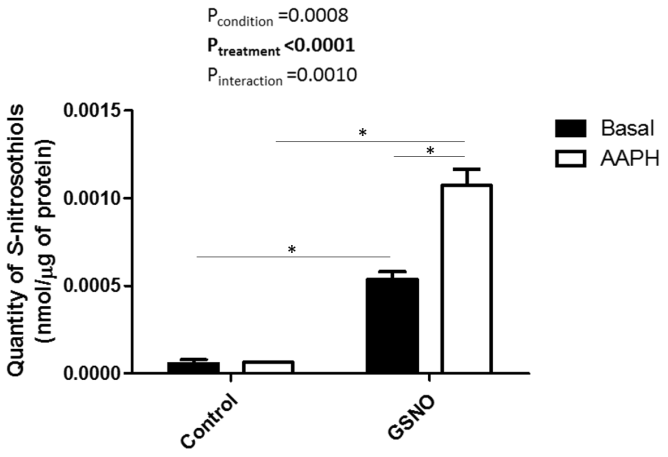

Fig. 5. Intracellular formation of *S*-nitrosothiols. Intracellular *S*-nitrosothiols were quantified by the DAN-Hg^{2+} method after incubation of smooth muscle cells for 3 h without (basal) or with 50 mM of AAPH. In each condition, 50 µM GSNO or GSNO+AAPH were added during the 3rd hour of incubation. Results are presented as means ± sem of three independent experiments and compared using a two way ANOVA ($p_{condition}$ (Basal *vs* AAPH), $p_{treatment}$ (Control, GSNO) and $p_{interaction}$); * $p < 0.05$ (Bonferroni's multiple comparisons test).

3.4. Identification of S-nitrosated proteins

Purification and identification of proteins undergoing *S*-nitrosation revealed that 68 proteins were nitrosated under basal conditions, whereas 83 were *S*-nitrosated under oxidative stress. GSNO-nitrosated proteins were mainly present in cell compartments entitled cell part including cytosol, cell junction proteins and nucleus, organelle and macromolecular complexes both under basal and oxidative stress conditions **(Table 1)**.

Table 1. Distribution of *S*-nitrosated proteins among distinct cell compartments upon treatment with GSNO (50 µM) of smooth muscle cells cultured under basal or oxidative stress (50 mM AAPH) conditions. Proteins were classified using the Panther database

	Percentage of total identified proteins	
Cell compartment	**Basal + GSNO**	**AAPH+GSNO**
Cell part	47.8	48.2
Membrane	1.5	1.2
Macromolecular complex	17.9	16.9
Organelle	31.3	32.5
Extracellular region	1.5	1.2

The identified proteins belonged to 18 different classes for both conditions. However, a class of transporter proteins is only represented under basal condition, and a class of lyase is only represented under oxidative stress **(Fig. 6)**.

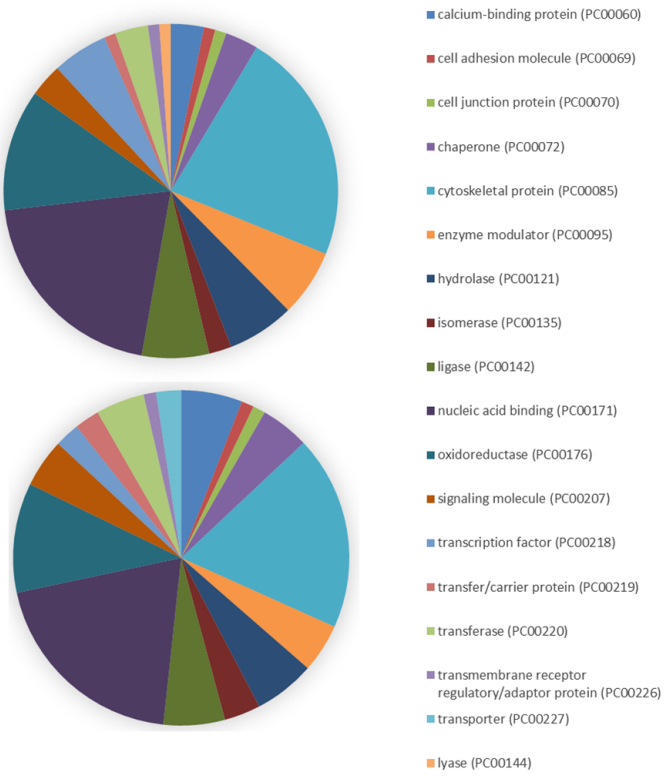

Fig. 6. Identification and classification of smooth muscle cells proteins *S*-nitrosated in basal or oxidative stress conditions. Proteins were *S*-nitrosated by 50 µM GSNO in cells exposed or not to oxidative stress (50 mM AAPH). After purification (biotin switch technique), proteins identified by mass spectrometry were classified using the Panther database.

In both culture conditions, the two major classes of *S*-nitrosated proteins were nucleic acid binding transcription factors and cytoskeletal proteins. Nucleic acid binding transcription factors accounted for 20% of identified proteins in basal conditions – with 17 different proteins including elongation factor 2 or cellular nucleic acid-binding protein – and 20.4% of identified proteins under oxidative stress with 19 different proteins. *S*-nitrosoglutathione induced *S*-nitrosation of a high proportion of SMC contractile proteins: 9 different cytoskeletal proteins were identified in basal conditions, and additional 6 (total: 9+6 = 15) under oxidative stress. Such proteins are structural constituents of cytoskeleton variably implicated in muscle contraction, as well as in cell morphogenesis and movement **(Table 2).**

Table 2. Molecular function and biological implications of cytoskeletal proteins *S*-nitrosated by 50 µM GSNO under basal or oxidative stress conditions.

Basal + GSNO	AAPH + GSNO	Molecular function	Biological process
Elongation Factor 1-Gamma		Structural constituent of cytoskeleton	Cell communication
	Actin, Aortic Smooth Muscle		Movement and morphogenesis and organization Mitosis
Alpha-Actinin-1		Structural constituent of cytoskeleton Actin binding	Movement
Calponin-2			Movement and morphogenesis and organization
Filamin-A			
Filamin-C			
	Lipoma-Preferred Partner	Structural constituent of cytoskeleton	Muscle contraction Movement
Myosin Regulatory Light Chain			Morphogenesis and organization
Talin-1			Movement, organization and morphogenesis Mitosis
Transgelin		Structural constituent of cytoskeleton Actin binding	Movement, organization and morphogenesis Muscle contraction
	Tubulin Beta-2a Chain	Structural constituent of cytoskeleton	
	Lim Domain And Actin-Binding Protein 1		Movement, Morphogenesis, Organization
Pdz And Lim Domain Protein 5			Movement, organization and morphogenesis Muscle contraction
	Pdz And Lim Domain Protein 1	Cadherin binding involved in cell-cell adhesion Non-motor actin binding protein	Cell-cell adhesion
	Destrin	Non-motor actin binding protein	Actin filament depolymerization

Within these different proteins, the cysteines targeted by NO were identified. Most of proteins like actin, cytoplasmic 1, transgelin, tubulin beta-2a chain or Pdz and Lim domain protein 5 are *S*-nitrosated on the same cysteine residue under basal or oxidative stress conditions (**Table 3**). Others like elongation factor 1-gamma or filamin-C (FLN-C) showed supplementary cysteine residues *S*-nitrosated under oxidative stress or basal conditions, respectively. However, *S*-nitrosated cysteine residues are at a different position within calponin-2 (CNN2) or alpha-actinin-1 following oxidative stress. As member of the same protein family, filamin-A (FLN-A) and FLN-C or transgelin (TAGLN) and transgelin-2 (TAGLN2) sequences were aligned to decipher whether their *S*-nitrosated cysteines were conserved residues along protein sequences. In FLN-A, the C53 (basal condition) and C810 (oxidative stress condition) *S*-nitrosated residues are conserved cysteines numbered C47 and C806 in FLN-C sequence, respectively. Although, *S*-nitrosated C729 in FLN-C is conserved as C733 position in FLN-A sequence, this position is not *S*-nitrosated in FLN-A. All other identified *S*-nitrosated residues were non-conserved cysteines. In TAGLN and TAGLN2, only C38 is a conserved residue at the same place in the sequence of each protein.

Table 3. Identification of cysteine *S*-nitrosated by 50 µM GSNO under basal and oxidative stress condition. Bold numbers highlight *S*-nitrosated cysteines place in the sequence

		Basal + GSNO	**AAPH + GSNO**
Protein name	**Total number and position of cysteines**	***S*-nitrosated cysteines**	
Elongation Factor 1-Gamma	N=6 68,166,**194**,210,266,**339**	194	194,339
Actin, cytoplasmic 1	N=6 17,**217**,257,272,285,374	217	
Alpha-Actinin-1	N=10 **41**,**154**,**180**,263,332,370,476,**480**,690,**774**,860	41,180, 154	180,480,774
Calponin-2	N=8 61,164,**175**,204,**215**,**240**,274,299	175,215	240
Filamin-A	N=50 8,**53**,59,205,210,444,478,483,574,623,631,649,717,733,796,**810**, **841**,1018,1108,1114,1122,1157,1165,1185,1198,1225,**1260**,1312, 1353,1402,1410,1453,1645,1686,1689,1723,1865,1912,1920,1997, 2102,2107,2160,2199,2293,2378,2476,2479,2582,2601	53,841,1260	810,841,1260
Filamin-C	N=46 **47**,53,199,204,439,473,478,536,619,627,645,666,**683**,713,**729**,792, 806,1014,1067,1104,1110,1118,1181,1349,1398,1406,1449,**1470**, 1640,1654,1681,1736,1763,1907,1915,1992,2089,2097,2102,2155, 2370,2455,2553,2556,2661,2680	47,683,729,1470	683
Myosin regulatory light chain RLC-A	N=1 **109**	109	
Transgelin	N=1 **38**	38	
Transgelin-2	N=3 38,**63**,124	63	
Tubulin Beta-2a Chain	N=7 **12**,127,129,211,**239**,303,354	12, 239	
Pdz And Lim Domain Protein 5	N=22 73,190,**213**,415,418,441,444,462,465,474,477,497,500,503,521,533,536,558,561,564,565,582	213	

Finally, six proteins were found to be *S*-nitrosated exclusively under oxidative stress (**Table 4**). Within the majority of these proteins, only one cysteine residue, upon 6 to 38 total cysteine residues for each protein, was affected by *S*-nitrosation. Pdz and lim domain protein 1 was the only protein showing two *S*-nitrosated cysteine residues over 8 total cysteine residues in its sequence.

Table 4. Identification of cysteine *S*-nitrosated by 50 µM GSNO only under oxidative stress condition. Total number and position of cysteines coming from the UniProt database with *S*-nitrosated positions in bold

Protein name	Total number and position of cysteines	*S*-nitrosated cysteines
Destrin	N=6 12,23,**39**,46,80,147	39
Actin, Aortic Smooth Muscle	N=7 2,12,19,**219**,259,287,376	219
Lim Domain And Actin-Binding Protein 1	N=12 140,164,229,314,342,388,391,**412**,415,418,436,562	412
Pdz And Lim Domain Protein 1	N=8 45, **73**, 258, 261, 281, 284, 287, **305**	73,305
Talin-1	N=38 29,116,236,243,286,336,575,709,719,732,**750**,956, 1023,1045,1087,1199,1202,1353,1363,1392,1434, 1478,1486,1506,1509,1558,1661,1671,1927,1939, 1953,1978,2161,2196,2219,2243,2408,2442	750
Lipoma-Preferred Partner	N=28 134,259,265,**301**,361,436,439,450,461,464,467, 485,488,496,499,519,522,525,539,544,556,559, 586,589,592,604,613,616	301

4. Discussion

The present study was designed to evaluate the bioactivity of GSNO in vascular SMC exposed to oxidative stress. Experiments were thus planned in order to assess the efficiency of GSNO-dependent NO release, and to verify possible quantitative/qualitative changes induced by oxidative conditions in cellular protein *S*-nitrosation.

From an experimental point of view, two main approaches can be used to induce oxidative stress, *i.e.* either by inhibiting cellular antioxidant defenses or by increasing the free radical load. The latter can be obtained by exposing cells to extracellular ROS like $O_2^{\bullet-}$ or H_2O_2. Prolonged enzymatic generation of $O_2^{\bullet-}$ can be sustained *e.g.* by the xanthine/xanthine oxidase system, which however can introduce a major bias in the results, as itself can denitrosate *S*-nitrosothiols [34]. H_2O_2 prooxidant effects are mediated by the formation of hydroxyl radical, $^{\bullet}OH$, through the transition metal-catalyzed Fenton reaction. However, transition metals are also known to catalyze direct degradation of *S*-nitrosothiols, preventing transition metals and H_2O_2 use in our study. On the other hand, the water soluble azocompound 2,2'-azobis(2-amidinopropane) dihydrochloride(AAPH) can be considered as a 'clean' and reproducible free radical generator, as one mole of AAPH spontaneously decomposes at 37°C into one mole of nitrogen and two moles of carbon-centered radicals. AAPH-derived radicals can either combine with each other to produce a stable product, or react with molecular oxygen to generate peroxyl radicals ($ROO^{\bullet}$), or with polyunsaturated lipids of cell membranes thus starting lipid peroxidation [35]. A number of studies have employed AAPH to investigate antioxidant defenses in cellular systems [36, 37]. More recently, cytotoxic and genotoxic effects of $ROO^{\bullet}$ originating downstream of AAPH have been studied in a human microvascular endothelial cell line [38]. The effects of oxidative stress on the development of the cardiovascular system were also investigated after administration of AAPH in the air chamber of chicken embryos [39]. As far as SMC are concerned, AAPH was

used (similar conditions to our study) to investigate the direct effects of free radicals on cyclic AMP-related cholesterol homeostasis [40]. On this background, the exposure of vascular SMC to AAPH was chosen as a simple and reproducible model of oxidative stress.

In our experiments, oxidative stress (in the absence of added GSNO) caused both a decrease in intracellular GSH and in SH groups of intracellular proteins, accompanied by an increase in extracellular GSH. The latter can be the result of AAPH-induced increase of GSH efflux as it was previously shown in erythrocytes challenged with H_2O_2, another oxidative stress inducer [41]. This increase in extracellular GSH concentration can be interpreted as a protection against the already known capacity of AAPH to directly oxidize plasma membrane proteins [42]. This speculation is confirmed in our work by the absence of variation of reduced thiol quantity at the plasma membrane of smooth muscle cells stress under AAPH challenge. GSH extracellular increase can also be due to the AAPH-induced decrease in GGT activity at the SMC plasma membrane level, which will lower the consumption of extracellular GSH. In fact, the AAPH-induced decrease of GGT activity can be explained as the effect of either direct inactivation of the enzyme protein by AAPH radicals or the large increase in the extracellular redox potential. Loss of cellular GGT activity was also reported following exposure of lung epithelial cells to hyperoxia-induced lipid peroxidation [43], and indeed, AAPH is known to induce lipid peroxidation [44].

Even if GGT activity is decreased by the AAPH-induced oxidative stress, the extracellular GSNO metabolism did not significantly change, as the consumption of added GSNO and the corresponding NO release were similar to basal conditions. In principle, the GSNO degradation might ensue from a direct oxidation by AAPH radicals. However, when checked in the absence of cells, the direct AAPH-mediated oxidation of GSNO (50 μM) actually released 4 ±0.1 μM nitrite ions, *i.e.* much less than the concentrations detected in the

presence of SMC (18.3±0.6 µM), suggesting that most of the observed GSNO metabolism in oxidative stress conditions in SMC occurs through the activity of diverse cellular enzymes.

Oxidative stress increased the formation of intracellular *S*-nitrosothiols under GSNO addition, and GGT inhibition decreased it. GGT is a critical enzyme in GSNO metabolism [45], essential for the release of NO and its subsequent utilization in *S*-nitrosothiols formation. Here, we showed that, even if the GGT activity decreased under oxidative stress, it was still implicated in GSNO extracellular catabolism and intracellular *S*-nitrosothiols formation, in the same extent than under basal conditions. Actually, GGT inhibition did not entirely suppress GSNO metabolism, as it could not restore the initial extracellular concentration of GSNO: approx. 27 µM GSNO were detected at the end of the incubation with GGT inhibitor, *vs* 20 µM without inhibition and *vs* 50 µM initially added. Taken together, these findings indicate that GGT activity is certainly involved in the extracellular metabolism of GSNO, but other enzymes must also be implicated in this process. As regards with PDI, similar results were obtained: enzyme inhibition did not entirely suppress GSNO extracellular metabolism and approx. 28 µM GSNO (*vs* 20 µM without inhibition and 50 µM initially added) were detectable in the extracellular compartment at the end of incubation. Cellular GGT and PDI activities appear therefore to remain implicated in GSNO catabolism, even if they were inversely impacted by oxidative stress (GGT activity decreases, while PDI expression at the membrane level increases).

The observed increase in *S*-nitrosation of SMC proteins under oxidative stress conditions is rather unexpected, as prooxidants should oxidize reduced thiols to disulfides and/or other sulfur species, which may be then unavailable for *S*-nitrosation thus interfering with NO-based physiologic signaling [46]. Furthermore, in principle, the addition of GSNO in an oxidative stress environment would rather be expected to enhance oxidative stress by the production of peroxynitrite anions. However in our system, AAPH induces the production of

intracellular peroxynitrite anion concentration (6.7 ± 0.8 µM, using dihydrorhodamine 123 probe), but the concomitant addition of GSNO did not modify this concentration (5.9 ± 0.4 µM). Moreover, it has been showed that *S*-nitrosation is a NO-protection from oxidation of thiols [47].

This was confirmed, in our system, by the reversion of AAPH-induced decrease of protein -SH groups under GSNO condition. The protection offered by GSNO to intracellular protein -SH groups could be explained by the release of GSH concomitantly to the release of NO. Released GSH can be incorporated after digestion into the intracellular GSH pool to support GSH-dependent antioxidant defenses. However, our data did not show any recovery of intracellular GSH levels after GSNO addition, probably due to direct oxidation of GSH by AAPH challenge. Therefore, the ability of GSNO to protect reduced protein thiols from oxidative stress, making them again available to react with NO, may represent the mechanism explaining the increased formation of intracellular *S*-nitrosothiols observed under oxidative conditions.

Protein *S*-nitrosation is considered as an important mechanism for post-translational modulation of protein function, and several studies have described such modulatory effects on a series of cys-containing proteins, being potential targets of RNS-dependent nitrosative modifications [48-50]. In addition to direct modulation of protein function, protein *S*-nitrosation can also represent a mean for constitution of a 'NO store' in tissues. Indeed, different studies support the idea that *S*-nitrosation of tissue thiols is a mechanism for the constitution of local reservoirs from which biologically active NO can be subsequently released [51-53]. Identification and assessment of such NO stores could provide a valuable biomarker for evaluation of the therapeutic efficiency of NO donors.

The increase in *S*-nitrosation mostly concerned proteins belonging to plasma membrane and extracellular region, which is not surprising considering that the AAPH-

dependent oxitative challenge was originated in the extracellular compartment. In particular, the detailed pattern of *S*-nitrosated proteins indicates that most of the proteins selectively *S*-nitrosated under oxidative stress conditions are of primary relevance for the performance of SMC functions, which are often altered in vascular diseases, such as cell communication, cytoskeletal organization, contraction, morphogenesis and movement.

Interestingly, the pathway involves actin cytoskeleton dynamics of several key regulatory proteins including CNN2, Myosin Regulatory Light Chain (MRLCA), TAGLN and Lipoma Preferred Partner (LPP). The role of *S*-nitrosation in regulating these proteins is not completely understood particularly during oxidative stress. Each of these proteins has been shown to play a role in regulating and modulating smooth muscle contraction or nitric oxide signaling. *In vitro S*-nitrosation of skeletal muscle myosin, for example, increases the force of the actomyosin interaction while decreasing its velocity indicating a relaxed state [54]. The calcium binding protein CNN2 has been shown to participate in regulating smooth muscle contraction by binding to actin, calmodulin, troponin C and tropomyosin. The interaction of calponin with actin inhibits the actomyosin Mg-ATPase activity [55, 56]. This tonic inhibition of the ATPase activity of myosin in smooth muscle is blocked by Ca^{2+}-calmodulin, which inhibits CNN2 actin binding [57]. MRLCA regulates smooth muscle and non muscle cell contractile activity and it does bind calcium. TAGLN (also designated SM22α and p27) is a smooth muscle protein that physically associates with cytoskeletal actin filament bundles in contractile SMC. Studies in transgelin knockout mice have demonstrated a pivotal role for transgelin in the regulation of Ca^{2+} independent contractility [58] and it is proposed to be necessary for actin polymerization and bundling [59]. Moreover, LPP, only found *S*-nitrosated under oxidative stress, is a nucleocytoplasmic shuttling protein, located in focal adhesions and associates with the actin cytoskeleton [60]. LPP can function as an adaptor protein that constitutes a platform that orchestrates protein-protein interactions and

contributes to the migratory phenotype of SMC [61]. As ROS have also been shown to enhance cell migration [62, 63] and GSNO has been shown to decrease SMC migration capacity [64], we can speculate that LPP *S*-nitrosation could protect against oxidative stress induced cell migration. Other proteins were also found *S*-nitrosated only under oxidative stress suggesting a difference of cysteine accessibility for NO under oxidative stress. This increase in cysteine accessibility can be managed under oxidative stress by redoxins like PDI and thioredoxin (Trx), whose activities are known to be increased under oxidative stress to reduce disulfide bounds formed by oxidant attacks. Furthermore, Trx activity was shown to be increased by GSNO [65] thus explaining the rise of intracellular thiols, which was found under GSNO added to our oxidative stress model. Indeed, our results showed an increase of PDI expression both at the plasma and organelle membranes level. Furthermore, PDI is known to catalyse transnitrosation reaction, so an increase in PDI activity by oxidative stress will probably lead to an increase in disulfide bound reduction and transnitrosation processes catalyzed by PDI. These extra *S*-nitrosated proteins included destrin, lim domain and actin-binding protein 1 (LIMA1) and talin-1 (TLN1). Destrin is a member of actin-binding family (ADF) proteins such as cofilin its isoprotein [66]. Destrin severs actin filaments (F-actin) and binds to actin monomers (G-actin) for actin depolymerization. It was shown that ADF family protein is responsible for F-actin dismantling through a redox-driven mechanism [67]. So, we can speculate that the *S*-nitrosation of destrin only under oxidative stress condition will interfere with actin filament severing through a redox mechanism. LIMA1 binds to actin monomers and filaments and inhibits actin filament depolymerization. LIMA1 expression was found significantly downregulated in cancers compared with normal tissues enhancing cancer cell invasion [68]. LIMA1 was also shown to be downregulated by oxidative stress [69] suggesting that the *S*-nitrosation observed only under oxidative stress in our experiments is a premise of a possible regulation of LIMA1 downregulation. Finally, TLN1 is involved in

connections of major cytoskeletal structures to the plasma membrane. TLN1 is one of the major constituents with vinculin of focal adhesion contributing to cellular well-being and intercellular communication. It was found downregulated in instable atherosclerotic plaques [70] which opens speculation on its implication in tissue disintegration in atherosclerotic plaques driven by loss of interactions among cells of the extracellular matrix and remodeling of the tissue. As atherosclerosis is a context of oxidative stress and NO depletion, we can speculate that *S*-nitrosation of TLN1 found under oxidative stress could help to restore TLN-1 activity.

The identification of *S*-nitrosated cysteines showed different or same repartition within protein structure depending on proteins considered. Some cysteine residues were *S*-nitrosated in both conditions because they are the only cysteine within the protein structure, so cannot form an intraprotein disulfide bound. Furthermore, some proteins present an odd number of cysteine residues in their sequence, so the *S*-nitrosated one is probably never implicated in intraprotein disulfide bound formation. In some proteins like calponin-2 the *S*-nitrosated cysteine residues are at different positions within the protein sequence probably because of disulphide bound rearrangement during oxidative stress challenge. Filamin-C showed four cysteine residues *S*-nitrosated by GSNO under basal condition and only one under oxidative stress. It is possible that lost *S*-nitrosated cysteine residues were oxidized by AAPH challenge.

Therefore, considered together, all these proteins, almost quite implicated in Ca^{2+}-dependent contractility, actin depolymerization and in NO signaling, constitute a potential interactome and discovering their behavior as *S*-nitrosated proteins may further help our understanding of several processes, such as contraction-relaxation signaling of SMC or their phenotype switching, in the vascular system.

In conclusion, our study documented that oxidative stress can significantly modify SMC metabolism of GSNO, an endogenous NO-donor presently under active investigation as

a potential therapeutic agent. In particular, oxidative stress was shown to increase the extent, and deeply modify the pattern of GSNO-dependent protein *S*-nitrosation, with the additional involvement in the process of several proteins critical for SMC homeostasis and function. These data can represent a valuable basis for the identification of biomarkers of GSNO bioactivity in the vascular system, as well as for the appraisal of possible beneficial effects of this NO donor in the treatment of CVD.

Acknowledgments

We thank the proteomics platform (Dr Jean-Baptiste Vincourt) and the imaging core facility (PTIBC IBISA Nancy) (Dr Dominique Dumas) from the Federation de Recherche (FR3209 CNRS - BMCT) based at the Biopôle on the biology-health campus at Université de Lorraine for the identification cysteines *S*-nitrosated in proteins (LC-MALDI MS) and for the formation and access provided to confocal imaging systems, respectively.

Funding

This work was supported by the *Université de Lorraine* and the *Région Lorraine* (UHP_2011_EA3452_BMS_0062, RL 21/11, RL 140/12, CPER 2007-13 PRST «Ingénierie Moléculaire et Thérapeutique – Santé »). Programme VINCI 2014 – Université Franco Italienne, project number C2-56 is also gratefully acknowledged.

References

[1] B.A. Maron, S.S.Tang, J. Loscalzo, S-Nitrosothiols and the S-Nitrosoproteome of the cardiovascular system, Antiox Redox Signal. 18 (2012) 270-287.

[2] R. Messin, G. Boxho, J. De Smedt, I.M. Buntinx, Acute and chronic effect of molsidomine extended release on exercise capacity in patients with stable angina, a double-blind crossover clinical trial versus placebo, J. Cardiovasc. Pharmacol. 25 (1995) 558-563.

[3] B.M. Bennett, Biotransformation of organic nitrates and vascular smooth muscle cell function, Trends Pharmacol. Sci. 15 (1994) 245-249.

[4] D. Morley, L.K. Keefer, Nitric oxide/nucleophile complexes: a unique class of nitric oxide-based vasodilators, J. Cardiovasc. Pharmacol. 22 (1193) S3-S9.

[5] E.A. Kowaluk, R. Poliszczuk, H.L. Fung, Tolerance to relaxation in rat aorta: comparison of an S-nitrosothiol with nitroglycerin, Eur. J. Pharmacol. 144 (1987) 379–383.

[6] A.R. Butler, C. Glidewell, J. McGinnis, W.I. Bisset, Further investigations regarding the toxicity of sodium nitroprusside, Clin. Chem. 33 (1987) 490–492.

[7] P.J. Henry, O.H. Drummer, J.D. Horowitz. S-nitrosothiols as vasodilators: implications regarding tolerance to nitric oxide-containing vasodilators, Br. J. Pharmacol. 98 (1989) 757–766.

[8] P.V. van Heerden, S. Sviri, K.F. Ilett, C.F. Lam, Inhaled diazeniumdiolates (NONOates) as selective pulmonary vasodilators, Expert Opin. Investig. Drugs 11(2002) 897–909.

[9] H. Al-Sa'doni, A. Ferro, S-nitrosothiols: a class of nitric oxide-donor drugs, Clin.Sci. 98 (2000) 507–520.

[10] K.F. Ricardo, S.M. Shishido, M.G. de Oliveira, M.H. Krieger, Characterization of the hypotensive effect of S-nitroso-N-acetylcysteine in normotensive and hypertensive conscious rats, Nitric Oxide, 7 (2002) 57–66.

[11] A.J. de Belder, R. MacAllister, M.W. Radomski, S. Moncada, P.J. Vallance, Effects of S-nitrosoglutathione in the human forearm circulation: evidence for selective inhibition of platelet activation, Cardiovasc. Res. 28 (1997) 691–694.

[12] M.W. Radomski, D.D. Rees, A. Dutra, S. Moncada, S-Nitroso-glutathione inhibits platelet activation in vitro and in vivo, Br. J. Pharmacol. 107 (1992) 745–749.

[13] E.J. Langford, A.S. Brown, R.J. Wainwright, A.J. Debelder, M.R. Thomas, R.E.A. Smith, M.W. Radomski, J.F. Martin, S. Moncada, Inhibition of platelet activity by S-nitrosoglutathione during coronary angioplasty, Lancet, 344 (1994) 1458–1460.

[14] S. Rajagopalan, S. Kurz, T. Münzel, M. Tarpey, B.A. Freeman, K.K. Griendling, D.G. Harrison, Angiotensin II-mediated hypertension in the rat increases vascular superoxide production via membrane NADH/NADPH oxidase activation. Contribution to alterations of vasomotor tone, J Clin Invest. 97 (1996) 8:1916-23.

[15] C. Kunsch, R.M. Medford, Oxidative stress as a regulator of gene expression in the vasculature, Circ. Res. 85 (1999) 753–766.

[16] K. Irani, Oxidant signaling in vascular cell growth, death, and survival: a review of the roles of reactive oxygen species in smooth muscle and endothelial cell mitogenic and apoptotic signaling, Circ. Res. 87 (2000) 179–183.

[17] K.K. Griendling, D. Sorescu, M. Ushio-Fukai, NAD(P)H oxidase: role in cardiovascular biology and disease, Circ. Res. 86 (2000) 494–501.

[18] G.N. Rao and B.C. Berk, Active oxygen species stimulate vascular smooth muscle cell growth and proto-oncogene expression, Circ. Res. 70 (1992) 593–599.

[19] M.W. Foster, D.T. Hess, J.S. Stamler, Protein S-nitrosylation in health and disease: a current perspective, Trends Mol Med. 15 (2009): 391-404.

[20] J.S. Paige, G. Xu, B. Stancevic, S.R. Jaffrey, Nitrosothiol reactivity profiling identifies S-nitrosylated proteins with unexpected stability, Chem Biol. 15 (2008) 1307-1316.

[21] A.J. Gow, Q. Chen, D.T. Hess, B.J. Day, H. Ischiropoulos, J.S. Stamler, Basal and stimulated protein S-nitrosylation in multiple cell types and tissues, J Biol Chem. 277 (2002): 9637-9640.

[22] H.J. Hsieh, C.A. Liu, B. Huang, A.H. Tseng, D.L. Wang, Shear-induced endothelial mechano transduction: the interplay between reactive oxygen species (ROS) and nitric oxide (NO) and the pathophysiological implications, J Biomed Sci, 21 (2014) 3.

[23] F. Dahboul, P. Leroy, K. Maguin Gate, A. Boudier, C. Gaucher, P. Liminana, I. Lartaud, A. Pompella, C. Perrin-Sarrado, Endothelial γ-glutamyltransferase contributes to the vasorelaxant effect of S-nitrosoglutathione in rat aorta, PLoS One. 7 (2012) 9:e43190.

[24] C. Gaucher, A. Boudier, F. Dahboul, M. Parent, P. Leroy, S-nitrosation/Denitrosation in Cardiovascular Pathologies: Facts and Concepts for the Rational Design of S-nitrosothiols, Curr. Pharm. Des. 19 (2013) 458-472.

[25] M. Parent, F. Dahboul, R. Schneider, I. Clarot, P. Maincent, P. Lerroy, A.Boudier, A complete physicochemical identity card of S-nitrosoglutathione, Curr Pharm Anal. 9 (2013): 31–42.

[26] C. Perrin-Sarrado, M. Pongas, F. Dahboul, P. Leroy, A. Pompella, I. Lartaud, Reduced Activity of the Aortic Gamma-Glutamyltransferase Does Not Decrease S-Nitrosoglutathione Induced Vasorelaxation of Rat Aortic Rings, Front Physiol. 7(2016) 630.

[27] W. Wu, C. Gaucher, R. Diab, I. Fries, Y.L. Xiao, X.M. Hu, P. Maincent, A. Sapin-Minet, Time lasting S-nitrosoglutathione polymeric nanoparticles delay cellular protein S-nitrosation, Eur J Pharm Biopharm. 89 (2015) 1-8.

[28] K. Lewicki, S. Marchand, L. Matoub, J. Lulek, J. Coulon, P. Leroy, Development of a fluorescence based microtiter plate method for the measurement of glutathione in yeast, Talanta, 70 (2006) 876–882.

[29] K. Maguin Gaté, I. Lartaud, P. Giummelly, R. Legrand, A. Pompella, P. Leroy, Accurate measurement of reduced glutathione in gamma-glutamyltransferase-rich brain microvessel fractions, Brain Res. 1369 (2011) 95-102.

[30] S.R. Jaffrey, S.H. Snyder, The biotin switch method for the detection of S-nitrosylated proteins, Sci STKE 86 (2001) pl1.

[31] S.R. Jaffrey, Detection and characterization of protein nitrosothiols, Methods Enzymol. 396 (2005) 105-118.

[32] M. Riffault, D. Moulin, L. Grossin, D. Mainard, J. Magdalou, J.B. Vincourt, Label-free relative quantification applied to LC-MALDI acquisition for rapid analysis of chondrocyte secretion modulation, J Proteomics. 114 (2015) 263-273.

[33] H. Mi, S. Poudel, A. Muruganujan, J.T. Casagrande, P.D. Thomas, PANTHER version 10: expanded protein families and functions, and analysis tools, Nucleic Acids Res. 44 (2016) D336-D342.

[34] M. Trujillo, M.N. Alvarez, G. Peluffo, B.A. Freeman, R. Radi, Xanthine oxidase-mediated decomposition of S-nitrosothiols. J Biol Chem. 273 (1998) 7828-7834.

[35] N. Noguchi, M. Takahashi, J. Tsuchiya, H. Yamashita, E. Komuro, E. Niki, Action of 21-aminosteroid U74006F as an antioxidant against lipid peroxidation. Biochem.Pharmacol. 55 (1998) 785-791.

[36] J.H. Yang, J.W. Park, Oxalomalate, a competitive inhibitor of $NADP^+$-dependent isocitrate dehydrogenase, enhances lipid peroxidation-mediated oxidative damage in U937 cells, Arch. Biochem. Biophys. 416 (2003) 31-7.

[37] G. Aldini, M. Carini, A. Piccoli, G. Rossoni, R.M, Facino Procyanidins from grape seeds protect endothelial cells from peroxynitrite damage and enhance endothelium-dependent relaxation in human artery: new evidences for cardio-protection, Life Sci. 73 (2003) 2883-2898.

[38] R. Scarpato, C. Gambacciani, B. Svezia, D. Chimenti, G. Turchi, Cytotoxicity and genotoxicity studies of two free-radical generators (AAPH and SIN-1) in human microvascular endothelial cells (HMEC-1) and human peripheral lymphocytes, Mutat Res. 722 (2011) 69-77.

[39] R.R. He, Y. Li, X.D. Li, R.N. Yi, X.Y. Wang, B. Tsoi, K.K. Lee, K. Abe, X. Yang, H. Kurihara, A new oxidative stress model, 2,2-azobis(2-amidinopropane) dihydrochloride induces cardiovascular damages in chicken embryo, PLoS One. 8 (2013):e57732.

[40] L .Gesquiere, N. Loreau, D. Blache, Role of the cyclic amp-dependent pathway in free radical induced cholesterol accumulation in vascular smooth muscle cells, Free Radic Biol Med. 29 (2000) 181–190.

[41] C. Muanprasat, C. Wongborisuth, N. Pathomthongtaweechai, S. Satitsri, S. Hongeng, Protection against oxidative stress in beta thalassemia/hemoglobin E erythrocytes by inhibitors of glutathione efflux transporters, PLoS One. 8 (2013):e55685.

[42] M. Soszyński, G. Bartosz, Decrease in accessible thiols as an index of oxidative damage to membrane proteins, Free Rad. Biol. Med. 23 (1997) 463-9.

[43] R.J. van Klaveren, J.L. Pype, M. Demedts, B. Nemery, Decrease in gamma-glutamyltransferase activity in rat type II cells exposed in vitro to hyperoxia: effects of the 21-aminosteroid U-74389G, Exp Lung Res. 23 (1997) 347-359.

[44] E. Niki, Free radical initiators as source of water- or lipid-soluble peroxyl radicals, Methods Enzymol. 186 (1990) 100-108.

[45] V. Angeli, A. Tacito, A. Paolicchi, R. Barsacchi, M. Franzini, R. Baldassini, C. Vecoli, A. Pompella, E. Bramanti, A kinetic study of gamma-glutamyltransferase (GGT)-mediated S-nitrosoglutathione catabolism, Arch Biochem Biophys. 481 (2009) 2: 191-6.

[46] T. Adachi, R.M. Weibrod, D.R. Pimentel, J. Ying, V.S. Sharov, C. Schoneich, R.A. Cohen, S-glutathiolation by peroxynitrite activates SERCA during arterial relaxation by nitric oxide, Nat Med. 10 (2004) 1200–120.

[47] J. Sun, C. Steenbergen, E. Murphy, S-nitrosylation: NO-related redox signaling to protect against oxidative stress, Antioxid Redox Signal. 8 (2006) 1693-1705.

[48] B. Huang, S.C. Chen, D.L.Wang, Shear flow increases S-nitrosylation of proteins in endothelial cells, Cardiovasc. Res. 83 (2009) 536–546.

[49] J. Hoffmann, S. Dimmeler, J. Haendeler, Shear stress increases the amount of S-nitrosylated molecules in endothelial cells: important role for signal transduction, FEBS Letters. 551 (2003) 153–158.

[50] H.E. Marshall, K. Merchant, J.S. Stamler, Nitrosation and oxidation in the regulation of gene expression. Faseb J. 14 (2000) 1889–1900.

[51] M. Sarr, M. Chataigneau, N. Etienne-Selloum, A.S. Diallo, C. Schott, M. Geffard, J.C. Stoclet, V.B. Schini-Kerth, B. Muller, Targeted and persistent effects of NO mediated by S-nitrosation of tissue thiols in arteries with endothelial dysfunction, Nitric Oxide. 17 (2007) 1-9.

[52] J.L. Alencar, I. Lobysheva, K. Chalupsky, M. Geffard, F. Nepveu, J.C. Stoclet, B. Muller, S-nitrosating nitric oxide donors induce long-lasting inhibition of contraction in isolated arteries, J. Pharmacol. Exp. Ther. 307 (2003) 152-159.

[53] W. Wu, C. Perrin-Sarrado, H. Ming, I. Lartaud, P. Maincent, X.M. Hu, A. Sapin-Minet, C. Gaucher, Polymer nanocomposites enhance S-nitrosoglutathione intestinal absorption and promote the formation of releasable nitric oxide stores in rat aorta, Nanomedicine. 16 (2016), pii: S1549-9634: 30053-3.

[54] A.M. Evangelista, V.S. Rao, A.R. Filo, N.V. Marozkina, A. Doctor, D.R. Jones, B. Gaston, W.H. Guilford, Direct regulation of striated muscle myosins by nitric oxide and endogenous nitrosothiols, PLoS One. 5 (2010) e11209.

[55] J.D. Carmichael, S.J. Winder, M.P. Walsh, G.J. Kargacin, Calponin and smooth muscle regulation, Can. J. Physiol. Pharmacol. 72 (1994) 1415–1419.

[56] S.J. Winder, B.G. Allen, O. Clement Chomienne, M.P. Walsh, Regulation of smooth muscle actinmyosin interaction and force by calponin, Acta Physiol. Scand. 164(1998) 415–426.

[57] M. Mezgueldi, C. Mendre, B. Calas, R. Kassab, A. Fattoum, Characterization of the regulatory domain of gizzard calponin. Interactions of the 145–163 region with Factin, calcium binding proteins, and tropomyosin, J. Biol. Chem. 270 (1995) 8867–8876.

[58] H.D. Je, U.D. Sohn, SM22alpha is required for agonistinduced regulation of contractility: evidence from SM22alpha knockout mice, Mol Cells, 23(2007) 175–181.

[59] M. Han, L.H. Dong, B. Zheng, J.H. Shi, J.K. Wen, Y. Cheng, Smooth muscle 22 alpha maintains the differentiated phenotype of vascular smooth muscle cells by inducing filamentous actin bundling, Life Sci. 84 (2009) 394-401.

[60] M.M. Petit, J. Fradelizi, R.M. Golsteyn, T.A. Ayoubi, B. Menichi, D. Louvard, W.J. Van de Ven, E. Friederich, LPP, an actin cytoskeleton protein related to zyxin, harbors a nuclear export signal and transcriptional activation capacity, Mol. Biol. Cell. 1 (2000) 117–129.

[61] I. Gorenne, L. Jin, T. Yoshida, J.M. Sanders, I.J. Sarembock, G.K. Owens, A.P. Somlyo, AV. Somlyo, LPP expression during in vitro smooth muscle differentiation and stent-induced vascular injury, Circ Res. 98 (2006) 378-385.

[62] J. Kim, G. Min, Y.S. Bae, D.S. Min, Phospholipase D is involved in oxidative stress-induced migration of vascular smooth muscle cells via tyrosine phosphorylation and protein kinase C, Exp Mol Med. 36 (2004) 103–109.

[63] L. Jin, M.J. Kern, C.A. Otey, B.R. Wamhoff, A.V. Somlyo, Angiotensin II, focal adhesion kinase, and PRX1 enhance smooth muscle expression of lipoma preferred partner and its newly identified binding partner palladin to promote cell migration, Circ. Res. 100 (2007) 817–825.

[64] P. Simmers, A. Gishto, N. Vyavahare, C.R. Kothapalli, Nitric oxide stimulates matrix synthesis and deposition by adult human aortic smooth muscle cells within three-dimensional cocultures, Tissue Eng Part A. 21(2015) 1455-1470.

[65] P.C. Schulze, H. Liu, E. Choe, J. Yoshioka, A. Shalev, K.D. Bloch, R.T. Lee, Nitric oxide-dependent suppression of thioredoxin-interacting protein expression enhances thioredoxin activity, Arterioscler Thromb Vasc Biol. 26(2006) 2666-2672.

[66] H. Hatanaka, K. Ogura, K. Moriyama, S. Ichikawa, I. Yahara, F. Inagaki, Tertiary structure of destrin and structural similarity between two actin-regulating protein families, Cell. 85 (1996) 1047-55.

[67] E.E. Grintsevich, H.G. Yesilyurt, S.K. Rich, R.J. Hung, J.R. Terman, E. Reisler, F-actin dismantling through a redox-driven synergy between Mical and cofilin, Nat Cell Biol. 18 (2016) 876-85.

[68] T. Ohashi, M. Idogawa, Y. Sasaki, T. Tokino, p53 mediates the suppression of cancer cell invasion by inducing LIMA1/EPLIN, Cancer Lett. 390 (2017) 58-66.

[69] M. Succoio, M. Comegna, C. D'Ambrosio, A. Scaloni , F. Cimino, R. Faraonio, Proteomic analysis reveals novel common genes modulated in both replicative and stress-induced senescence, J Proteomics. (2015) 18-29.

[70] M. von Essen, R.Rahikainen, N. Oksala, E. Raitoharju, I. Seppälä, A. Mennander, T. Sioris, I. Kholová, N. Klopp, T. Illig, P.J. Karhunen, M. Kähönen,T. Lehtimäki, V.P. Hytönen, Talin and vinculin are downregulated in atherosclerotic plaque; Tampere Vascular Study, Atherosclerosis. 255 (2016) 43-53.